ISSN 0974-3618 (Print)
0974-360X (Online)

www.rjptonline.org

RESEARCH ARTICLE

Synthesis and characterisation of graphene oxide supported mono and bimetallic nano particles as catalyst with anti bacterial activity

Perumal Andal*, Chandran Loganayagi, Roopakala
Department of Chemistry, School of Basic sciences, Vels University, Pallavarm,
Chennai-600117,Kancheepuram District, Tamil Nadu, India.
*Corresponding Author E-mail: **andalprithu.sbs@velsuniv.ac.in**

ABSTRACT:
Nanoparticles have unique material characteristics, may find practical applications in a variety of areas, including medicine, engineering, catalysis and environmental remediation due to their ultrafine unit with dimensions measured in nanometres (nm; 1 nm = 10^{-9} metre). Nanoparticles are made by comminution (the pulverization of materials), such as through industrial milling or natural weathering, by pyrolysis (incineration), or by sol-gel synthesis (the generation of inorganic materials from a colloidal suspension). In this study two different types of graphene oxide supported two mono Ru, Pd, and a bimetallic Ru/Pd nanoparticles catalyst were synthesized. The size and shape of the products were characterized by various techniques such as : scanning electron microscopy (SEM), high resolution transmission electron microscopy (HRTEM) field emission scanning electron microscopy with edax (FESEM-EDAX) x-ray diffraction spectroscopy (XRD) Raman analyses followed by kinetic study. Results proved that the newly developed graphene oxide supported bimetallic nanoparticles catalysts can be more efficient to reductive, oxidative and of environmentally important organic pollutant additionally it is also very good biologically active compound.

KEYWORDS: Graphene Oxide(GO), Palladium, Rhodamine, nanoparticle.

INTRODUCTION:
Nanoparticles are particles having specific physical and chemical properties that are intermediate between those of the atomic element from which they are composed relative to those of the bulk metals [1]. Stabilization of high –index crystal planes and alternative packing arrangement of atoms can also occur in small nanoparticles [2]. Nanoparticles may consist of identical atoms, molecules and two or more different species. Nanoparticles have distinct properties from those of individual atoms and molecules or bulk matter, they found it as effective catalyst in olefin hydrogenation [3-4].

In the recent years, metal nanoparticles have attracted much attention owing to their excellent high activity against many species of bacteria and fungi [5–7]. These metal nanoparticles revealed the new optical, electrical, and mechanical properties and higher reactivity due to their high surface to volume ratio, distinct from those of the corresponding metallic bulk materials. Furthermore, bimetallic composite nanoparticles, composed of two different metal elements, are of a greater interest than monometallic nanoparticles from both scientific and technological points of view. The structure of bimetallic nanoparticles is defined by the distribution modes of the two elements and can be oriented in random alloy, alloy with an intermetallic compound, cluster-in-cluster, and core-shell structures, leading to enhanced applications, compared to monometallic nanoparticles [8–11].

Received on 19.07.2017 Modified on 20.08.2017
Accepted on 11.09.2017
Research J. Pharm. and Tech 2017; 10(10):3610-3620.
DOI: 10.5958/0974-360X.2017.00656.4

Beside with the characterization of the nanoparticles, molecular dynamical simulations for the structural and most stable structure of the Pt and Pd bimetallic nanoparticles have also been performed. Nanoparticles have a range of potential applications in various fields' like medicine, environment, energy, electronics, manufacturing of material etc[12-13]., Bimetallic (or multi metallic) catalysts have long been valuable for in-depth investigations of the relationship between catalytic activity and catalyst particle structure. The addition of a second metal can provide many benefits, such as enhanced activity, stability and greater control of selectivity. Graphene, an important two-dimension nanomaterial. It holds great promise for potential applications in many technological fields such as sensors, electronics, super capacitors, batteries, fuel cells, solar cells, nanocomposites, and hydrogen storage because of its high specific surface area, excellent thermal and electrical conductivity, and strong mechanical strength [14-18].

Compounds of Cr (VI) are proven to have high toxicities, mutagenicities and carcinogenicities, and are considered to be one of the most common pollutants at hazardous waste sites [19-20]. Nanoparticles (NPs) offer many advantages over conventional bulk catalysts by providing high surface area to volume ratio for better catalytic performance [21-26].

In the light of above advantages and considering the significance of the bimetal nanocatalyst the present study was mainly focused with the following objectives. It is proposed to synthesis of two different types of Graphene oxide-supported mono and bimetallic nanoparticles catalysts. Further the individual size characterization of each catalyst using different instrumental techniques Viz., UV-Visible, SEM, EDAX, HRTEM, XRD etc. The catalytic potential of the proposed two different method mono and bimetallic nanoparticles catalysts were part-A ascertained based on the pseudo first-order rate constant for the reduction of Rhodamine b and malachite green. Part-B comparative catalytic study of Go-supported mono and bimetallic nanoparticles for the reductive conversion of Cr(VI) to Cr(III) and catalytic reduction of eosin y and anti-bacterial activity.

MATERIALS:

Graphite powder (SRL), potassium tetrachloropalladatate (SRL), silver nitrate (SRL), ruthenium trichloride hydrate (SRL), potassium dichromate (SRL), Rhodamine b and Malachite green (SRL), sodium boro hydride (SRL), Eosin y (Alfa aesar), Formic acid (SRL), sodium hydroxide (Alfa aesar), ethanol (SRL), Double distilled water were analytical grade of 99% purity and used as received.

INSTRUMENTS AND CHARACTERIZATION:

UV-Visible spectrophotometer

The UV-vis spectra were measured on PerkinElmer Lamda-35 instruments with UV Win-lab software. The measurements were carried out in the wavelength range of 200-800 nm under ambient conditions.

SEM and EDAX

The surface morphology study was performed using JEOL JSM-6360 Scanning electron microscope (SEM). Since polymeric materials are electrically non-conducting, they should be made conducting by platinum coating. The samples were spread on the surface of double sided adhesive tape, one side of which was already adhered to surface of a circular copper disc pivoted by a rod.JEOL JSM -6360 auto fine-coating ion sputter was used for the platinum coating.

FESEM and HRTEM

Field emission scanning electron microscopy of the prepared GO supported nanoparticles was recorded on a SU6600, HITACHI model operating at an accelerating voltage of 100 kV instrument. The sample for analysis was prepared by taking equal amounts and spreading on the surface of double-sided adhesive tape, one side was already adhered to the surface of a circular copper disk pivoted by a rod and the spreaded samples were sputtered with gold prior to SEM observation. The respective sample was scanned with HRTEM using JEOL 3010 high-resolution transmission electron microscope (HRTEM) operated at 300 keV. Energy dispersive spectroscopy was performed on aEDS DX-4 energy diffraction spectrometer of the SEM and the observed percentage of elements was compared quantitatively.

Raman analysis

The Raman analysis was performed with E-ZRaman-H handheld Raman analyzer with desktop. The E-ZRaman-H Raman analyzers are ideal for various solid and liquid substance identification and authentication applications.

XRD

The powder X-ray diffraction patterns of the samples were recorded at room temperature on aBruker D8 Advance X-ray diffraction system with Cu Kα1 radiation.The X-ray photoelectron spectra were recorded in an ultra-high vacuum (UHV) chamber (evacuated to 3.5 X 10^{-10} mbar) of a photoelectron spectrometer Omicron nanotechnology, Germany (GmbH) equipped with a monochromatic X-ray source (AIKR hυ =1486.6 eV). The anode and filament were operated with 15 kV and 20 mA (300W) respectively.

Ultra Sonication

The ultra-sonication of each bimetal nanoparticles catalyst was done by cole-parmer sonication bath at 40keV and thus prepared the homogeneous solution for characterization and catalytic studies.

EXPERIMENTAL:

Graphite oxide was prepared by the using Hummer method and exfoliated into graphene oxide by sonication in water. These Go supported mono and bimetallic nanoparticles catalyst were prepared by chemical reduction method. The first catalyst viz., Ru-Pd bimetallic NPs was prepared by taking in a 100ml round bottom flask, typically, 0.06 mm of ruthenium trichloride hydrate to which potassium tetra chloropalladate was added. Sonicated (5 mg and 30ml water for 30 minutes) GO was added to the above mixture and the reaction was stirred for further 2 h at 120˚C. Finally 0.1 M sodium boro hydride solution was added to the reaction mixture. The resulting solution was cooled and centrifuged at 2500 rpm. The water and ethanol were used for further purification. The collected product was dried at 70˚C in vacuum oven.

In a similarly manner, by adopting the same quantity of the reagents and experimental procedure the bimetallic and mono metallic nanoparticles catalysts viz., Ru/Pd, Ru NPs were also prepared. The metal precursors for Ru/Pd, Ru were K_2PdCl_4, and $RuCl_3.H_2o$ solution. The reduction of Ru^{3+}, Pd^{2+} to Pd, Ru NPs was noticed through the change of color. The resulting two different bimetallic nanoparticles catalysts were characterized with SEM, FESEM-EDAX, HRTEM, Raman, XRD, and XPS analysis.

The comparative catalytic activity of mono and bimetallic nanoparticles catalysts were examined by conducting the reduction of Rhodamine B and Malachite green as well as Cr(IV) to Cr(III) a model reaction keeping under identical pseudo-first order experimental condition. The reaction was carried out individually in a standard quartz cuvette with 1 cm path length to which 2.5 ml water, 0.25 ml Rhodamine B and Malachite green (1 mmol), 0.25 ml $NaBH_4$ (100 mmol) and 5 mg of respective catalyst was added. Similarly the same reaction was followed instead of Rhodamine B and malachite green use 0.2 ml potassium dichromate ,1 ml of formic acid and 5 mg of GO-RU-PdNps respective catalyst was added. As well as the same reaction was followed in reduction of Eosin-Y. After mixing the respective solution the corresponding cuvette was placed in a UV-vis spectrometer maintaining the temperature at 27°C.The occurrence of the reaction was recorded in the range from 200-700 nm, for example the UV-vis spectrum recorded for Go-Ru-Pd NPs catalyst was shown in fig.9 and 11the characteristic peaks for the reduction of Rhodamine B and Malachite green was observed at 544 nm and 617 nm which in turn followed gradually decreased through UV-vis spectrometer. The decreasing trend of characteristic peak was recorded at regular intervals of time (5min) and the same has been used for the calculation of pseudo first order rate constant. The pseudo first rate constant was calculated using the formula.

$$\mathbf{K_{obs} = ln[A\infty - A_0)/(A\infty - At)]/t}$$

Where,

$\mathbf{A\infty}$ -absorbance at infinity time, $\mathbf{A_0}$-initial absorbance, $\mathbf{A_t}$-absorbance at different time t.

The comparative K_{obs} values are calculated for another one bimetallic and three mono metallic nanoparticles catalysts .

The observed K_{obs}value reveals that the Go-Ru/Pd NPs catalyst is found to be superior catalysts compare to other bimetallic and mono metallic nanoparticles. Namely Ru/Pd, Ru NPs catalyst.

The anti-bacterial activity of graphene oxide supported mono and bimetallic nanoparticles catalysts was tested against four bacterial isolates such as Staphylococcus aureus, Escherichia coli, Salmonella typhi and Bacillus subtilis using Agar well diffusion method. Nutrient Agar plates were inoculated with 100 µL of standardized culture (1.5 108 CFU/mL) of each bacterium (in triplicates) and spread with sterile swabs. Wells of 6 mm size are made in the Agar plates containing the bacterial lawn. From the synthesized graphene oxide supported Ru-Ag bimetallic nanoparticles 50, 100 and 150 µg volume was poured into the wells made in the bacterial culture plates. The plates thus prepared were left at room temperature for ten minutes for allowing the diffusion of the extract into the agar bacterial lawn. After incubation for 24 h at 37 ˚C, the plates were observed.

RESULT AND DISCUSSION:

It is well known that the research on catalysis is proved to be a vital subject and this effort in turn can strengthen the economy of the industries. In the last two decades the research interest on development of homogeneous nanoparticles catalyst has increased tremendously owing to its and unaccountable advantages. Many reports have already appeared covering the synthesis of various mono and bimetallic nanoparticles catalyst for either oxidation or reduction of organic substrates. To synthesis homogeneous mono/bimetallic nanoparticles catalysts, one should need an appropriate template to stabilize/encapsulate the metal nanoparticles. Further in the preparation of homogeneous metal nanoparticles as

catalyst, identification of template/stabilizing agent is proved to be a bigger task.

It is also learned from the earlier studies that stabilization/encapsulation of bimetallic/mono metallic nanoparticles using single template has shown an excellent catalytic activity due to co-operative/synergetic effect of more than one metal nanoparticles. Similarly, although reduction of organic dyes, heavy metal ion and anti-bacterial activity are already studied with other existing catalysts but also far, there is no report available for effective reduction of the said substrate using heterogeneous catalyst that contains more than one metal nanoparticle as a catalyst. It is in this background, the present study deals with synthesis of two different methods of graphene oxide supported mono and bimetallic nanoparticles catalysts viz., Ru/Pd, Pd, and Ru Graphene oxide is a common stabilizing agent and K_2PdCl_4 and $RuCl_3.3H_2O$ as a metal precursor for Pd NPs, Ru NPs metal nanoparticles through simplified procedures. The obtained two different methods of mono and bimetallic nanoparticles catalysts were characterized with SEM, FESEM, EDAX, HRTEM, Raman and XRD analyses.

The comparative catalytic efficiency of two different types of mono and bimetallic nanoparticles catalysts were examined by conducting the reduction of organic dyes, heavy metal ion keeping under identical pseudo first order condition in the presence of $NaBH_4$ and formic acid. The occurrence of the reduction of Rhodamine b, Malachite green and heavy metal ion and Eosin y in the presence of bimetallic nanoparticles catalysts was confirmed from the appearance of the characteristic peaks for the product at 544 nm, 617 nm, 348 nm and 520 nm in the corresponding UV-vis spectra as shown in Figs. 1, 2, 3 and 4.

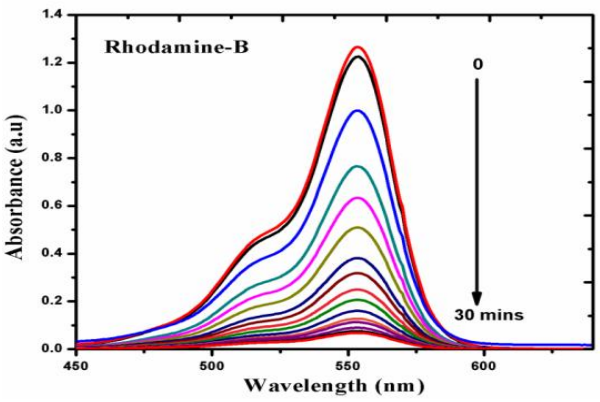

Figure 1.UV-vis spectrum for the reduction of Rhodamine-B using GO-Ru-Pd bimetallic NPs catalysts

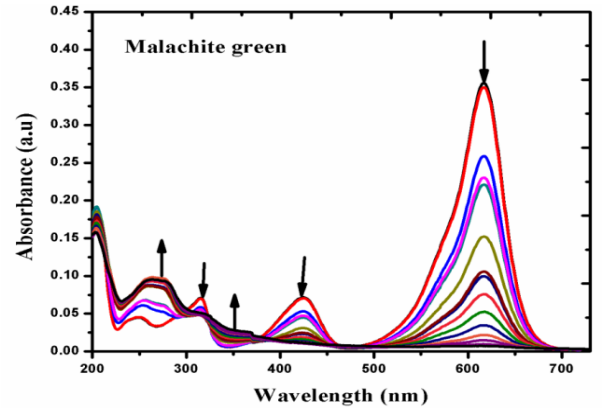

Figure 2.UV-vis spectrum for the reduction of malachite green using GO-Ru-Pd bimetallic NPs catalysts

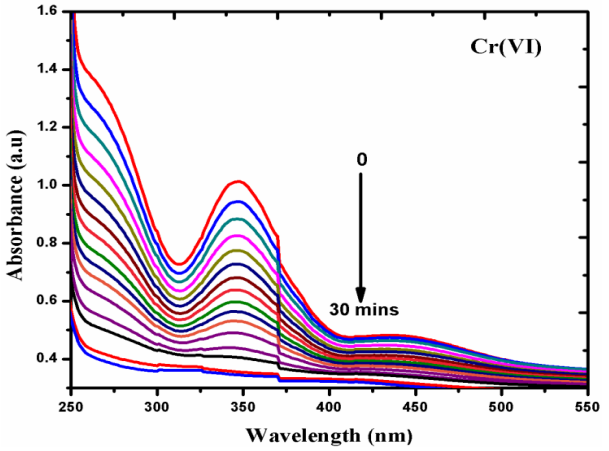

Figure 3.UV-vis spectrum for the reduction of Cr(VI) to Cr(III) using GO-Ru-Pd bimetallic NPs catalysts

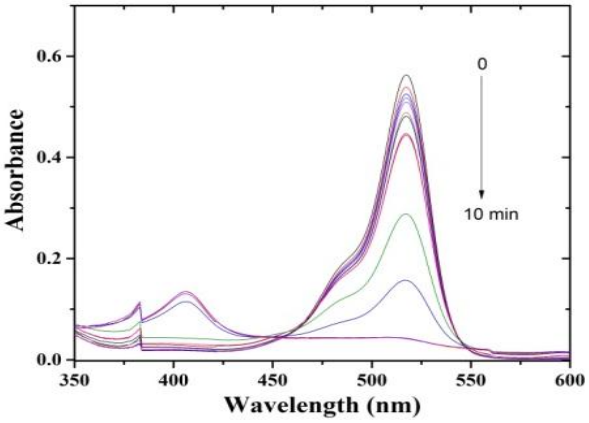

Figure 4. UV-vis spectrum for the reduction of eosin y using GO-Ru-Pd bimetallic NPs catalysts

Part-A Graphene Oxide supported mono and bimetallic nanoparticles

Nanoscale materials have attracted significant scientific and industrial interest. Considerable effort has been devoted to nanocomposite studies, i.e. alloy and core-shell nanoparticles, because of their valuable properties which make them useful for composition-dependent

optical application and catalysis. In the usual metal catalyst, addition of other element can often improve the catalytic activity and selectivity, from the same view point mono and bimetallic nanoparticles are also often investigated. Bimetallic nanoparticles retain an ever greater degree of catalytic activity than the mono metallic ones.

The simple approaches for the fabrication of GO-supported mono as well as bimetallic NPs were synthesized by co-reduction method using $NaBH_4$ in aqueous medium. The catalysts of GO supported bimetallic NPs were synthesized in three steps. In the first step, the graphene was converted in to graphene oxide by using hummer's method. The synthesis of stable nanoparticles was very difficult without any stabilizing agent. So before adding sodium boro hydride the metal ions and mixture was stirred at least 2 h. In step two then the colloidal metal ions solution was injected in to the GO solution under stirring condition. Finally, the sodium boro hydride solution was added drop wise in to the above mixture. The reaction was further continues for 30 minutes in the third step. The obtained products viz., mono and bimetallic NPs were characterized by SEM, FESEM, HRTEM, EDAX, Raman and XRD, spectroscopy. The catalytic efficiency of the newly developed NPs was studied for the reduction of organic dyes as a model reaction. The reduction reaction was monitored by using UV-visible techniques and the reusability of the superior catalyst was examined up to 3 cycles for the same reduction reaction.

The surface morphology of these mono metallic nanoparticles catalysts was performed by SEM analysis and the observed results are compared with corresponding polymer control that is the SEM image was found to be smooth in surface without any heterogeneity. In contrast the Pd, and Ru NPs obtained from figure 5 and 6 were reveals that irrespective of the images, there is an evenly distributed white dot have appeared on the surface of mono metallic NPs. This must be a contribution of formation of evenly distributed NPs on the surface of the spherical shape. Based on the results monometal nanoparticles are well supported by GO.

The surface morphology of GO supported bimetallic alloy NPs were investigated by using FESEM analysis. Figure.7 shows the surface morphology of GO supported Ru-Pd NPs. It clearly indicates that the spherical shape of Ru-Pd NPs was supported by GO. Based on the above results, the bimetallic alloy NPs is well supported by GO.

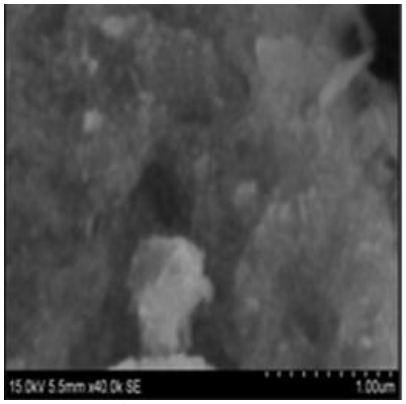

Figure 5. SEM images of GO-Pd

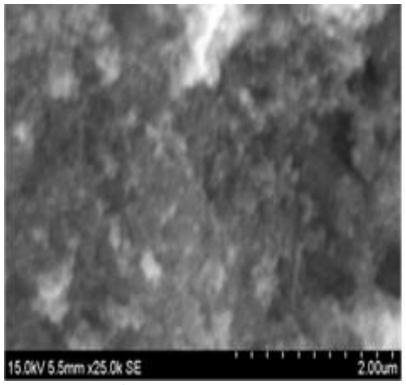

Figure 6. SEM images of GO-RuNps

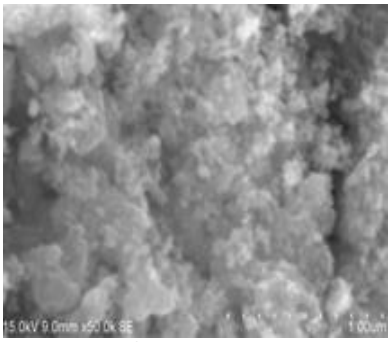

Figure 7.FESEM images of GO-Ru-Pd bimetallic NPs

EDAX

The weight percentage of Pd, Ru, and Ru-Pd alloy NPs were determined by EDAX analysis (Figure. 8, 9 and 10). From the EDAX measurement, the mono GO supported Pd NPs contain 17.2wt% of Pd and Ru NPs contain 34.50wt % of Ru. GO supported bimetallic Ru-Pd alloy NPs contain 48.7wt% of Ru and 7.30 wt% of Pd alloy NPs respectively**.**

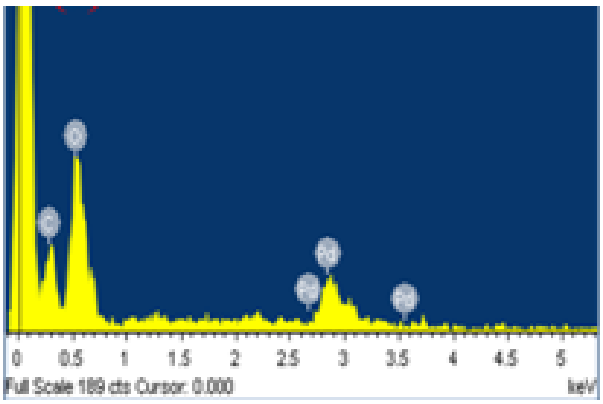

Figure 8. EDAX spectra of GO-Pd

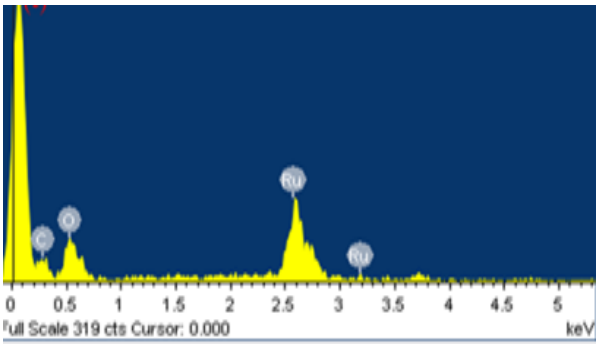

Figure 9. EDAX spectra of GO- Ru NPs

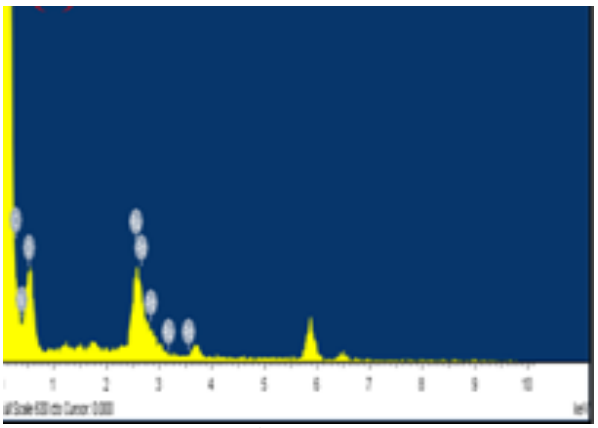

Figure 10. EDAX spectra Of GO-Ru-Pd bimetallic NPs

Raman spectral analysis

The Raman spectra of graphene oxide the D band around 1354 cm-1 and G band around 1549 cm-1 the obtained spectra confirm the formation of graphene oxide. (Figure11.)The Raman spectra of GO supported mono Pd, Ru NPs and bimetallic Ru-Pd alloy NPs. The D band around at 1360 cm^{-1} and G band around at 1608 cm^{-1} were observed for the all GO supported mono NPs as well as bimetallic alloy NPs (Figure12,13 and 14). It suggested that the GO are well supported for the deposition of mono NPs and bimetallic alloy NPs.

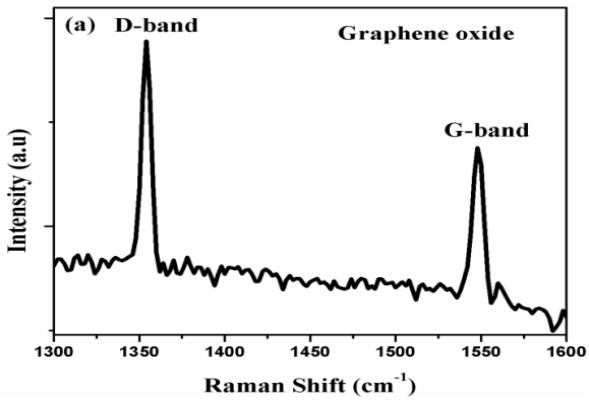

Figure 11.Raman spectra of GO

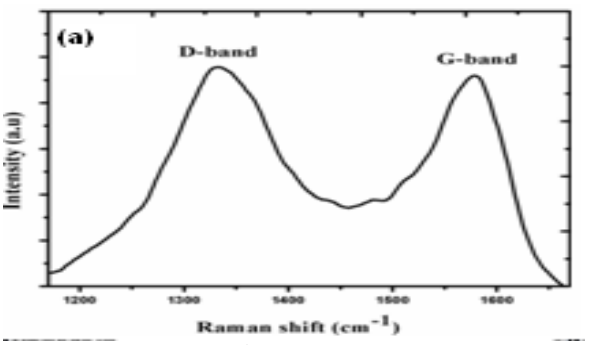

Figure 12. Raman spectra of GO-Pd

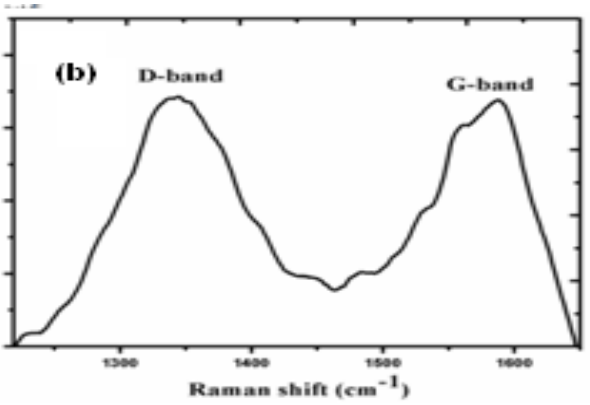

Figure 13. Raman spectra of GO- Ru

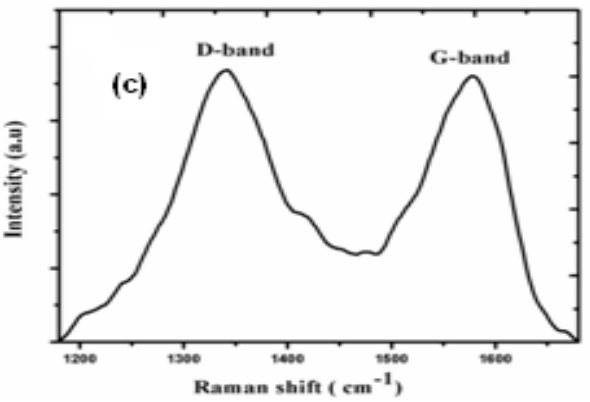

Figure 14. Raman spectra of GO-Ru-Pd bimetallic NPs

HRTEM

The particle size and shape of the GO supported bimetallic alloy NPs were investigated by using HRTEM analysis. Figure 15 shows, the HRTEM images of GO supported Ru-Pd NPs, and it clearly mentions that the particles are spheres with 10 nm size. Based on the above results, the prepared bimetallic alloy NPs is uniformly distributed on the GO surface. It should be noted that almost no NPs can be observed outside of the GO sheets which indicates that the GO serves here as a template for NPs formation. Based on the above results, the GO act as a very good supporting agent for mono as well as bimetallic alloy NPs.

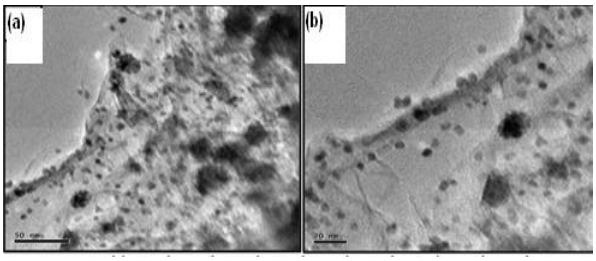

Figure 15. HRTEM images of (a-b) GO-Ru-Pd bimetallic NPs

XRD

The GO supported bimetallic Ru-Pd alloy NPs were obtained after centrifugation and the dried samples were analyzed by powder XRD to determine their crystalline nature and particles size with 2θ values between 20 to 80 ºC. Figures 16 showed the characteristic peaks for crystalline mono and bimetallic Ru-Pd NPs.

Further the characteristic 2θ values at 39 º, 47.4º, 66.1º, 69.3º 79.6º and 83.9ºfor Ru-Pd NPs are corresponds to 111, 200, 220, 220,311and 222 planes. These peaks confirm the formation of Ru-Pd the formation of which is in good agreement with the JCPDS files no 88- 2333 and 87-0637 Ru-Pd NPs. Moreover, there is no additional impurity peaks were observed, which indicates only crystalline mono and bimetallic NPs are present. Based on the above results, the mono as well as bimetallic Ru-Pd alloy NPs are well supported by GO.

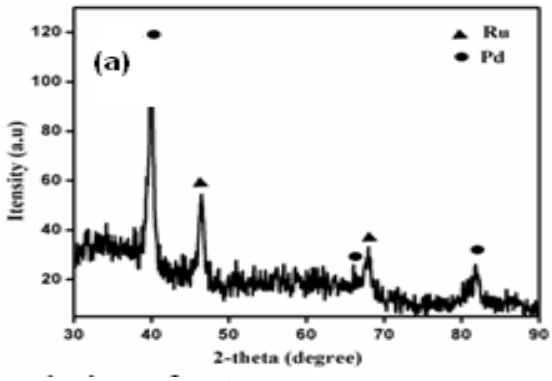

Figure 16. XRD spectra of GO-Ru-Pd bimetallic NPs catalysts

Comparative catalytic effect of mono and bimetallic nanoparticles catalysts for the reduction of Organic Dyes

The comparative catalytic effect of mono and bimetallic nanoparticles catalysts such as Pd, and Ru NPs for monometallic nanoparticles and Ru-Pd NPs for bimetallic nanoparticles was studied using reduction of organic dyes as a model reaction under pseudo first order identical condition. Figure 17 and 18 shows representative successive UV-visible spectra of the reduction of Rhodamine b and Malachite green in the presence of $NaBH_4$.

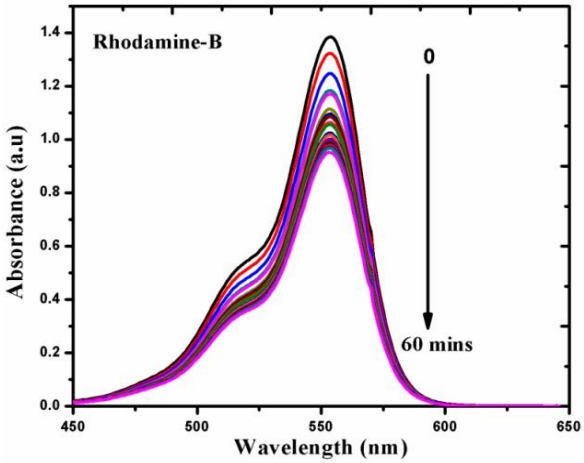

Figure 17. UV-vis spectrum for the reduction of Rhodamine-B using $NaBH_4$(Control)

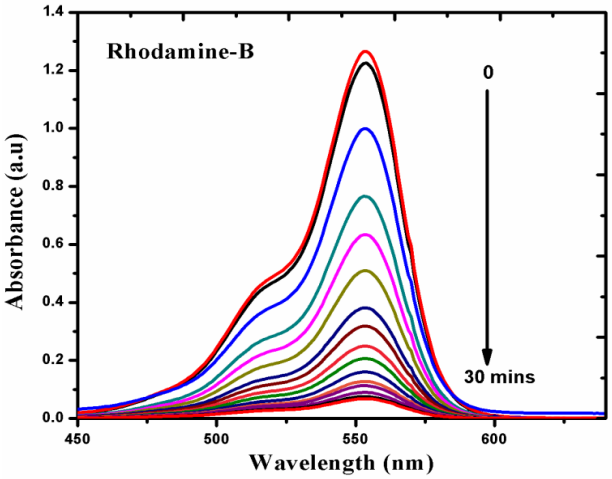

Figure 18. UV-vis spectrum for the reduction of malachite green using $NaBH_4$ (Control)

Without catalysts there is slightly decrease of Rhodamine b and Malachite green dyes in figure. 17 and 18. Additionally Figure. 19 and 20 shows in the presence of catalysts the peak gradually decreased at 544 nm and 617 nm. The comparative catalytic reduction of pseudo first order rate constants for the

reduction of rhodamine b and malachite green are given the table no.1 and 2.

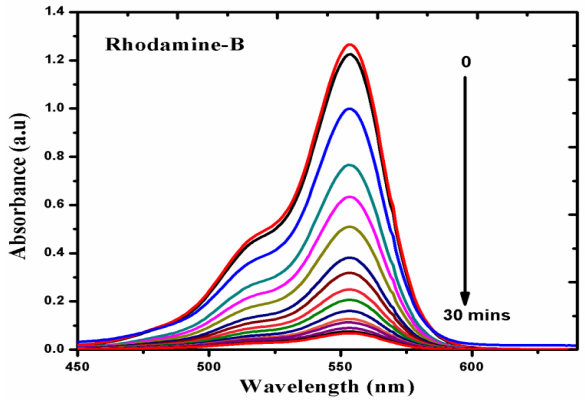

Figure 19 UV-vis spectrum for the reduction of Rhodamine-B using GO-Ru-Pd NPs catalysts

From the K_{obs}results, the order of the rate constant is Pd, Ru, and Ru-Pd NPs. The observed rate constant for the reduction of Rhodamine b and Malachite green using Ru-Pd NPs k_{obs} =1.67x10^{-3}S^{-1} and 1.6024x10^{-3}S^{-1} was found to be higher than other bimetallic nanoparticles and mono metallic nanoparticles catalyst as shown in Table.1 & 2. The reason for increased k_{obs} noticed in Ru-Pd NPs may be attributed to the following reactor that is, from the HRTEM studies, it is understood that size distribution of the Ru-Pd NPs catalyst was found to be relatively smaller 10 nm than another catalyst viz.

Table 1. Comparative catalytic activity for Rhodamine-B reduction

S. No	Name of the catalyst	K_{obs} x10^{-3}s^{-1}
1.	GO-Ru NPs	1.47 x 10^{-3}s^{-1}
2.	GO-Pd NPs	1.67 x 10^{-3}s^{-1}
3.	GO-Pd NPs	1.67 x 10^{-3}s^{-1}

Table 2. Comparative catalytic activity for Malachite green reduction

S. No	Name of the catalyst	K_{obs} x10^{-3}s^{-1}
1.	GO-Ru NPs	0.4934
2.	GO-Pd NPs	0.5721
3.	GO-Ru/Pd NPs	1.6024

Kinetic study for the reduction of Rhodamine-B using Graphene Oxide supported Ru-Pd NPs catalyst

In order to know the effect of [NaBH4], [substrate] and [Catalyst] on the reduction of organic dyes, the superior catalyst viz., Ru-Pd NPs was employed and studied under pseudo-first order reaction condition. As usual, the kinetics of the dyes reduction reaction was followed by measuring the absorbance of the product with decreasing trend 544 nm against the time through UV-vis spectrophotometer. From the observed rate constants, it is understood that the [NaBH4], [substrate] and [Catalyst] has been largely influenced the kobs in the reduction of organic dyes substrate.

Effect of [substrate]

The substrate concentration was varied from 0.8 to 1.4 mm at constant temperature 27^{o}C and the experiments were performed by maintaining the other parameters as constant. The rate constants are calculated from the plot of 2+log (Aα-At) *vs* time and the calculated values are given in Table 3, The observed rate constants are decreased consistently on increasing the dyes. The decreasing trend of rate constant is due to lesser availability of BH_4- in aqueous phase and thus minimizing the formation of product.

Table 3.Effect of the substrate

S.no	[Rh-B] mm	[$NaBH_4$] mm	[Catalyst]mg	K_{obs}x 10^{-3}s^{-1}
1.	0.8	100	5	80
2.	1.0	100	5	1.97
3.	1.2	100	5	1.59
4.	1.4	100	5	1.39

Effect of [$NaBH_4$]

The effect of concentration of $NaBH_4$ for reduction of rhodamine b was studied in the range from 60 to 110 mm keeping the other parameters as constants. From the plot of 2+log (Aα-At) *vs* time, the pseudo-first order rate constants were evaluated and presented in Table 4 and the corresponding plots were depicted in Figure 20.The observed rate constants increased with the increase in the concentration of $NaBH_4$. On increasing the [$NaBH_4$], the adsorption of BH_4- ions onto the nanoparticles surfaces also parallely increases, as a result, the relay of electrons from BH_4^- (donor) to the Rh-b (receptor) increases. It is worth to state that under the fixed concentration of $NaBH_4$the reduced product viz., organic dyes is not oxidized further because, the liberated hydrogen from boro hydride purged out the air has prevented the oxidation. In addition, evolution of small bubbles of hydrogen on the catalyst surface helped in mixing of the solution and thus offering the favorable conditions to increase the reaction rates.

Table 4.Effect of the $NaBH_4$

S.no	[Rh-B] mm	[$NaBH_4$]mm	[Catalyst]mg	K_{obs}x 10^{-3}s^{-1}
1.	1.0	60	5	1.41
2.	1.0	80	5	1.72
3.	1.0	100	5	1.97
4.	1.0	110	5	3.72

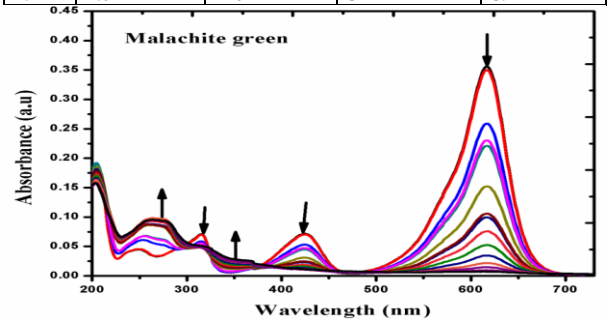

Figure 20 UV-vis spectrum for the reduction of malachite green using GO-Ru-Pd NPs catalysts

Effect of catalysts

Similarly, in the case of effect of [catalyst] variation, the kobs were found to increase on increasing the concentration of catalyst irrespective of organic dyes substrate. To examine the effect of GO- Ru-Pd NPs, the said reduction of organic dyes reaction was performed by varying the catalyst amount from 3 mg to 8 mg given table5 keeping the other parameters constant. The plot derived from observed rate constant against the amount of catalyst is shown in Figure. 21 from this plot, it is understand that on increasing the amount of catalyst, the rate constant are also parallely increased. This is quite obvious that at higher load of catalyst amount, the active nanoparticles is also available largely that contributed enhanced rate constant.

Table 5.Effect of the catalyst

S. no	[Rh-B] mm	[$NaBH_4$]mm	[Catalyst]mg	$K_{obs}x10^{-3}s^{-1}$
1.	1.0	100	3	1.37
2.	1.0	100	5	1.97
3.	1.0	100	7	2.81
4.	1.0	100	8	4.11

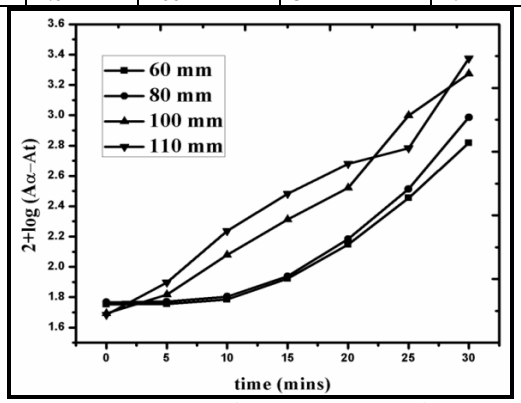

Figure 21.Consolidated plot for the reduction of Rhodamine-B catalyzed by GO-Ru-Pd bimetallic NPs catalysts

Kinetic study for the reduction of malachite green using Graphene Oxide supported Ru-Pd NPs catalyst
Effect of [$NaBH_4$]

The effect of concentration of $NaBH_4$ for reduction of malachite green was studied in the range from 60 to 110 mm keeping the other parameters as constants. From the plot of 2+log (Aα-At) *vs* time, the pseudo-first order rate constants were evaluated and presented in Table. 6 and the corresponding plots was depicted in figure 22.The observed rate constants increased with the increase in the concentration of $NaBH_4$. On increasing the [$NaBH_4$], the adsorption of BH_4- ions onto the nanoparticles surfaces also parallely increases, as a result, the relay of electrons from BH_4- (donor) to the MG(receptor) increases. It is worth to state that under the fixed concentration of $NaBH_4$ the reduced product viz., organic dyes is not oxidized further because, the liberated hydrogen from boro hydride purged out the air has prevented .

Table 6.Effect of [$NaBH_4$]

S.no	[MG] mm	[$NaBH_4$]mm	[Catalyst]mg	$K_{obs}x\ 10^{-3}s^{-1}$
1.	1.0	60	5	0.63
2.	1.0	80	5	0.68
3.	1.0	100	5	1.60
4.	1.0	110	5	1.89

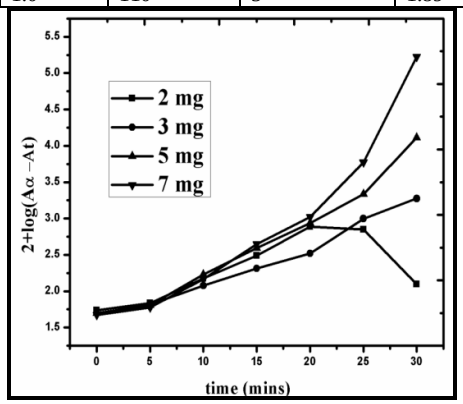

Figure 22.Consolidated plot for the reduction of malachite green by Go catalyzed Ru-Pd bimetallic NPs catalysts

Effect of [catalysts]

Similarly, in the case of effect of [catalyst] variation, the kobs were found to increase on increasing the concentration of catalyst irrespective of organic dyes substrate. To examine the effect of GO-Ru-Pd NPs, the said reduction of organic dyes reaction was performed by varying the catalyst amount from 2 mg to 7 mg given table 7 keeping the other parameters constant.The plot derived from observed rate constant against the amount of catalyst is shown in figure 22. From this plot, it is understand that on increasing the amount of catalyst, the rate constant are also parallely increased. This is quite obvious that at higher load of catalyst amount, the active nanoparticles is also available largely that contributed enhanced rate constant.

Table 5. Effect of [Catalyst]

S.no	[MG] mm	[$NaBH_4$]mm	[Catalyst]mg	$K_{obs}x\ 10^{-3}s^{-1}$
1.	1.0	100	2	1.89
2.	1.0	100	3	1.60
3.	1.0	100	5	2.18
4.	1.0	100	7	2.58

ANTI-BACTERIAL ACTIVITY

Further the graphene oxide supported mono as well as bimetallic nanoparticles catalyst by using anti-bacterial activity. Two strains including Gram negative E. coli, and Salmonella typhimurium and Gram-positive Bacillus subtilis and Staphylococcus aureus were selected for antibacterial tests because they are usually associated with the medical-associated infections. The comparative Anti-bacterial property of GO-Ru-Pd, GO-

Pd, and GO-Ru nanoparticles was investigated by calculating anti-bacterial ratios based on the numbers of bacteria colonies incubated with different dosages of GO-supported mono and bimetallic nanoparticles at 37 °C after a contact time of 1 h, as shown in Figure. 23.

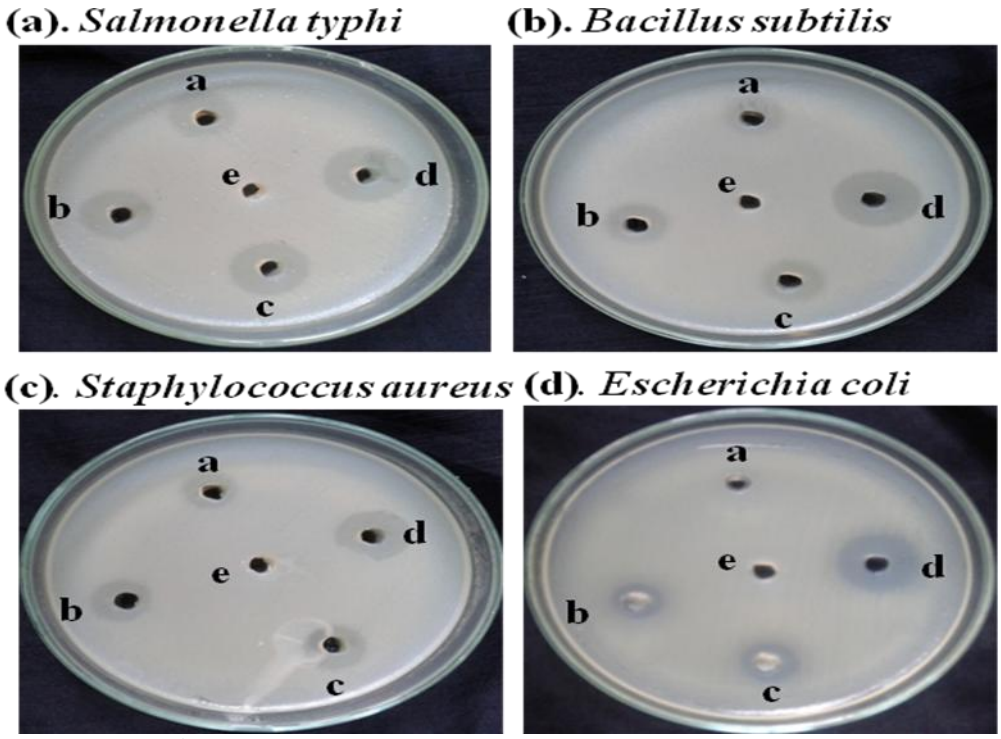

Figure 23. Anti-bacterial activity of GO-Ru-Pd bimetallic NPs catalysts
a-50mg, b-100mg, c-150mg, d-25mg

CONCULSION:

Different types of graphene oxide supported two mono Ru, Pd, and bimetallic Ru/Pd nanoparticles catalyst. The obtained both mono and bimetallic nanoparticles catalysts were shape and size characterized by using various techniques such as : scanning electron microscopy (SEM), high resolution transmission electron microscopy (HRTEM) field emission scanning electron microscopy with edax (FESEM-EDAX) x-ray diffraction spectroscopy (XRD) Raman analyses.Further, the catalytic potential of these two different types of mono and bimetallic nanoparticles catalysts using various reactions. Part-A graphene oxide supported mono and bimetallic nanoparticles using catalytic reduction of various organic dyes and part-B graphene oxide supported mono and bimetallic nanoparticles using catalytic reductive conversion of Cr (VI) and reduction of Eosin y and anti-bacterial activity.From the observed results it reveals that the newly developed graphene oxide supported bimetallic nanoparticles catalysts can be more efficient to reductive, oxidative and of environmentally important organic pollutant additionally it is also very good biologically active compound.

REFERENCES:

1. Anthony. J.L, Maginn. E.J, Brennecke,Solubilities and thermodynamics Properties of gases ,*Journal of physical chemistry B*, 106(29), 2002 ,7315-7320.
2. Tian N, Zhou Z. Y, Sun S. G,platinum Metal catalysts of High – Index Surface from single crystal planes to Electrochemically Shape-controlled nanoparticles, *Journal of physicalchemistry* C 112(50), 2008, 19801-19817.
3. Riccardo Ferrando, Julius Jellinek ,Roy L Johnson,From the theory of application of alloy clusters and Nanoparticles, *Chemical Reviews*, 108(3), 2008,846-910.
4. MarccialM ,Roser P, Fromation of carbon-carbon bonds wide catalysis by transition metal nanoparticles ,*Accounts Chemical Research*, 36(8), 2003, 638-643.
5. HajipourM. J, FrommK. M, Akbar Ashkarran A et al., Antibacterial properties of nanoparticles, *Trends in Biotechnology*, 30(10) 2012,499–511.
6. Rai M, Yadav A, and Gade A, "Silver nanoparticles as a new generation of antimicrobials, *Biotechnology Advances*, 27(1), 2009, 76–83,.
7. Patel B.Hand Chattopadhyay D.P, Preparation, characterization and stabilization of nanosized copper particles, *International Journal of Pure and Applied Sciences and Technology*, 9(1), 2012, 1–8,.
8. Kim N .R, Shin K., Jung I, Shim M, and Lee H.M,Ag-Cu bimetallic nanoparticles with enhanced resistance to oxidation: a combined experimental and theoretical study," The *Journal of Physical Chemistry C*, 118(45), 2014, 26324–26331,.

9. Sopoušek J, Pinkas J, Brož P et al, Ag-Cu colloid synthesis: bimetallic nanoparticle characterisation and thermal treatment, *Journal of Nanomaterials*, 2014, 13 pages, 2014.
10. Sarkar A, Mukherjee T, and Kapoor S, "PVP-stabilized copper nanoparticles: a reusable catalyst for 'click' reaction between terminal alkynes and azides in nonaqueous solvents, *The Journal of Physical Chemistry C*, 2008,112(9), 3334–3340.
11. Kidwai M, Mishra N.K , Bansal V, Kumar A, and Mozumdar S, Cu-nanoparticle catalyzed O-arylation of phenols with aryl halides via Ullmann coupling, *Tetrahedron Letters*, 48(50), 8883–8887, 2007.
12. HolbreyJ, and Seddon K. R,Ionic Liquid,*Clean Prodceeding. Processes*. 1(4), 1999,223–236.
13. Seddon K.R. Ionic Liquids for Clean Technology,*Journal of Chemical Technology Biotechnology*,68(4), 1997, 351–356.
14. L. Xiao and K. E. Johnson, " *Electrochemistry of 1-Butyl-3-methyl-1H-imidazolium Tetrafluoroborate Ionic Liquid*" J*ournal of Electrochemistry Society*, 150, (6)2003,307-307 .
15. P. Vanysek, *CRC Handbook of Chemistry sand Physics*, CRC Press, Boca Raton 82 (2001-2002) 1032.
16. Wilkes J.S, Zaworotko M.J ,Air and water stable 1-ethyl-3-methylimidazolium based ionic liquids ,*Chemical Communications* (13)1992965-967.
17. Walker A.J and Bruce N.C,Cofactor-dependent enzyme catalysis infunctionalized ionic solvent , *Chemical Communications*99 (22),2004, 2570 - 2571.
18. EarleM. J, EsperançaJ. M.S.S, GileaM. ACanongia Lopes J. N,RebeloL. P.N, Magee J.W, Seddon K. R. and WidegrenJ. A, The distillation andvolatility of ionic liquid,*Nature*,439,2006,831-834.
19. Y.Y.Liu and Xiong, Y. 'Purification and characterization of a dimethoate-degrading enzyme of Aspergillus niger ZHY256 isolated from sewage', *Applied andEnvironmentalMicrobiology*, 67, (8)2001,3746–3749.
20. Ludwig R.D, Lee.S.C, Wilkin R.T, Acree S.D, Ross R.R,Insitu chemical reduction of Cr(VI) in groundwater using a combination of ferrous sulphate and sodium dithionite: a field investigation', *Journal of Environmental Science and Technology*, 41, (15)2007,5299–5305.
21. QuinnJ, Geiger C, Clausen C, Brooks K, Coon C, Hara S, Krug T, Major D, Yoon W.S, Gavsakar A, and Holdsworth T, Field demonstration of DNAPL dehalogenation using emulsified zero-valent iron', *Environmental Science and Technology*, 39(5), 2005, 1309–1318.
22. H.H. Read, *Rutley's Elements of Mineralogy*, 26th ed., 1970,p.560,
23. ShakeelA.A, QayyumH, 'Potential applications of enzymes immobilized on/in nano materials: a review', *Biotechnology Advances*, 30(3), 2012, 512–523.
24. TaoL.C, and AndrewR, 'Encapsulation of nZVI particles using a Gum Arabic stabilized oil-in-water emulsion', *Journal of Hazardous Materials*, 189(3), 2011, 801–808.
25. YangX, Shen Z, Zhang B, Yang J, Hong W.X, Z.Zhuang, and Liu J, 'Silicananoparticles capture atmospheric lead: implications in the treatment of environmental heavy metal pollution', *Chemosphere*, 90(1), 2013, 653–656.
26. ZhangW.X, 'Nanoscale iron particles for environmental remediation: an overview', *Journal of Nanoparticle Research*, 37(5), 2003, 323–332.